BIOCHEMISTRY
including biophysical chemistry & molecular biology

Article

pubs.acs.org/biochemistry

How Hydrogen Peroxide Is Metabolized by Oxidized Cytochrome *c* Oxidase

Daniel Jancura,*[,†,∥] Jana Stanicova,[‡] Graham Palmer,[§] and Marian Fabian*[,∥,§]

[†]Department of Biophysics, University of P. J. Safarik, Kosice, Slovak Republic

[‡]Institute of Biophysics, University of Veterinary Medicine and Pharmacy, Kosice, Slovak Republic

[§]Department of Biochemistry and Cell Biology, Rice University, Houston, Texas 77251-1892, United States

[∥]Center for Interdisciplinary Biosciences, University of P. J. Safarik, Kosice, Slovak Republic

ABSTRACT: In the absence of external electron donors, oxidized bovine cytochrome *c* oxidase (CcO) exhibits the ability to decompose excess H_2O_2. Depending on the concentration of peroxide, two mechanisms of degradation were identified. At submillimolar peroxide concentrations, decomposition proceeds with virtually no production of superoxide and oxygen. In contrast, in the millimolar H_2O_2 concentration range, CcO generates superoxide from peroxide. At submillimolar concentrations, the decomposition of H_2O_2 occurs at least at two sites. One is the catalytic heme a_3−Cu_B center where H_2O_2 is reduced to water. During the interaction of the enzyme with H_2O_2, this center cycles back to oxidized CcO via the intermediate presence of two oxoferryl states. We show that at pH 8.0 two molecules of H_2O_2 react with the catalytic center accomplishing one cycle. In addition, the reactions at the heme a_3−Cu_B center generate the surface-exposed lipid-based radical(s) that participates in the decomposition of peroxide. It is also found that the irreversible decline of the catalytic activity of the enzyme treated with submillimolar H_2O_2 concentrations results specifically from the decrease in the rate of electron transfer from heme *a* to the heme a_3−Cu_B center during the reductive phase of the catalytic cycle. The rates of electron transfer from ferrocytochrome *c* to heme *a* and the kinetics of the oxidation of the fully reduced CcO with O_2 were not affected in the peroxide-modified CcO.

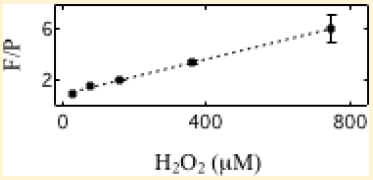

A basic molecular process in oxidative energy transformation is the coupling of redox reactions with transmembrane proton translocation. In mitochondria, this proton transfer is driven by redox reactions in three membrane-bound complexes: NADH-ubiquinone oxidoreductase, the bc_1 complex, and cytochrome *c* oxidase (CcO). Cytochrome *c* oxidases, members of the heme-copper oxidase superfamily, are multisubunit complexes that catalyze the reduction of oxygen to water and additionally pump protons across the mitochondrial inner membrane (for reviews, see refs 1−5). In isolated mammalian oxidases, the number of subunits is found to be as many as 13.[6] However, only two subunits harbor all four redox active cofactors.[7,8] Two copper centers, Cu_A and Cu_B, and two hemes, heme *a* and heme a_3, are located in subunits I and II and shielded from the solution by the protein matrix. In addition to the cofactors, purified CcO also contains a certain amount of protein-bound phospholipids.[9−12]

Under physiological conditions, Cu_A, a dinuclear copper site, is the initial electron acceptor from reduced cytochrome *c*. Subsequently, electrons flow from Cu_A to heme *a* and then to the catalytic binuclear heme a_3−Cu_B center where oxygen is reduced to water. The full reduction of O_2 to H_2O requires four electrons and four protons that are delivered sequentially to the catalytic site. Depending on the number of electrons and protons entering the heme a_3−Cu_B site, a series of discrete intermediates is observed. However, the reduction of O_2 can begin only when the enzyme is reduced by at least two electrons. The reaction product of two-electron-reduced CcO with O_2 is an intermediate called the "peroxy" form (**P**). An interesting feature of **P** is that the dioxygen bond is already cleaved[13,14] and the iron of heme a_3 is in the oxoferryl state (Fe_{a3}^{IV}=O).[13] It is assumed that splitting of the O−O bond in **P** is facilitated by the oxidation of an aromatic amino acid in the vicinity of the heme a_3−Cu_B center. It is probable that Tyr244 (bovine numbering) is the original electron or hydrogen donor producing the Tyr radical.[15−17] Entry of the third electron into the catalytic site converts **P** to the second ferryl form (**F**),[18−21] in which the Tyr radical is expected to be annihilated.[1] The full reduction of oxygen is completed by a delivery of the fourth electron to the catalytic center of **F**, regenerating the oxidized enzyme (**O**).

The catalytic sequence **O** → **P** → **F** → **O** is mimicked by the appearance of these intermediates during the treatment of the enzyme with H_2O_2.[22−26] The **P** state is formed by the interaction of the oxidized CcO with one molecule of H_2O_2.[27] A second molecule of H_2O_2 converts **P** to **F**.[26,28,29] In addition to these observations, it has been proposed that **F** can react with either the third H_2O_2 molecule[24] or a superoxide[1] to yield **O**. In the presence of excess peroxide, the enzyme shows the ability to continually decrease the concentration of H_2O_2 by turnover, even in the absence of external electron donors.[30] In the course of this turnover, the release of molecular oxygen

Received: August 8, 2013
Revised: May 19, 2014
Published: May 19, 2014

   dx.doi.org/10.1021/bi401078b | *Biochemistry* 2014, 53, 3564−3575

(O_2),[31−33] superoxide,[34,35] and hydroxyl radicals[36] has been observed. Moreover, CcO exposed to peroxide showed various sites of oxidative modifications and a decline in catalytic activity.[37−40] It has also been demonstrated that this oxidative damage is triggered by the reaction of H_2O_2 with the catalytic site of CcO.[37,38] These observations led to suggestions that the oxidized enzyme possesses the so-called pseudocatalase and/or endogenous peroxidase activity.[24,30,37,38]

Clearly, the characterization of the reactions of CcO with peroxide can assist in improving our understanding of the chemical nature of the two transient ferryl intermediates. Moreover, these investigations should be helpful in explaining the inhibition of the catalytic activity of CcO caused by H_2O_2 treatments. In this study, we have applied several kinetic and spectroscopic methods to identify the type of interactions of CcO with peroxide and the pathway of the oxidative damage and to demonstrate the specificity of peroxide attack on the catalytic electron transfer reactions.

EXPERIMENTAL PROCEDURES

Materials. Horseradish peroxidase (HRP), catalase, scopoletin, imidazole, ethylenediaminetetraacetic acid (EDTA), diethylenediaminepentaacetic acid (DEPA), Tris and Ches buffers, sucrose, L-histidine, hexaaminеruthenium(III) chloride (Ru), nitro blue tetrazolium type III (NBT), and sodium hydrosulfite (dithionite, DT) were purchased from Sigma-Aldrich. Horse heart ferricytochrome *c* was obtained from Fluka, 30% hydrogen peroxide from Fisher Scientific, sodium cyanide from Mallinckrodt, *n*-dodecyl *β*-D-maltoside (DM) from Anatrace, Triton X-100 from Roche Diagnostics, and the high-purity spin trap *α*-(4-pyridyl-1-oxide)-*N*-*tert*-butylnitrone (POBN) from Alexis Biochemicals.

CcO Purification and Activity Measurements. Bovine heart cytochrome *c* oxidase was isolated from mitochondria by the modified method of Soulimane and Buse[41] into DM-containing buffer [10 mM Tris (pH 7.6), 50 mM K_2SO_4, and 0.1% DM].[42] The concentration of the oxidized CcO was determined from the optical spectrum using an extinction coefficient A_{424} of 156 mM^{-1} cm^{-1}.[43] Using the published purification procedure,[41] we noticed that the pseudocatalase activity, the rate of production of O_2 from the reaction of H_2O_2 with the oxidized enzyme, varies with the CcO preparation. Because it has been suggested that the catalase-like function may reflect the action of adventitious transition metals on H_2O_2,[30] we have included one additional step in the isolation protocol. This step involved washing the first sediment obtained after solubilization of mitochondria with Triton X-100 with buffer [10 mM Tris (pH 7.6) and 250 mM sucrose] containing the chelators 10 mM EDTA and 5 mM histidine. This modified procedure yields CcO showing no measurable generation of O_2 from H_2O_2 assessed by the oxygen electrode.

Exposing the mitochondrial extract to 10 mM EDTA and 5 mM histidine during purification does not result in the observable deviation of the examined characteristics of CcO relative to those of the enzyme not exposed to the chelators. The tested properties included the optical spectra of the fully oxidized and fully reduced CcO, the reaction of the oxidized CcO with carbon monoxide to produce the "peroxy" intermediate under aerobic conditions, the rate of electron transfer (ET) from heme *a* to the heme a_3−Cu_B center during the anaerobic reduction of the enzyme, and the rates of reactions of the oxidized enzyme with both cyanide and H_2O_2. Because alteration of the catalytic properties and the catalytic center of CcO was not observed, we attributed the effect of the chelators to the removal or decrease of the concentration of some transition metals in solutions.

The catalytic activity of CcO was determined from the kinetics of the oxidation of 7 *μ*M ferrocytochrome *c* by 15 nM CcO monitored as the absorbance change at 550 nm in a Hewlett-Packard 8452 UV−vis spectrometer. Ferrocytochrome *c* was prepared by the reduction of the oxidized protein with a few crystals of solid dithionite, and then the solution was passed through a G25 column. The concentration of the reduced cytochrome *c* was calculated from the optical spectra using an A_{550} of 27.6 mM^{-1} cm^{-1}. To avoid any complexities of CcO aggregation during prolonged incubation at neutral pH, a buffer with a high ionic strength [200 mM potassium phosphate buffer (pH 7.0) and 0.1% DM at 23 °C] was used in most of the measurements.

Complex of CcO with Cyanide. The very high affinity of cyanide for oxidized CcO facilitates the preparation of the complex (CcO·CN) with no free cyanide in solution. This complex was formed by an incubation of the enzyme with 10 mM NaCN for 20 min in 200 mM potassium phosphate buffer (pH 7.0) and 0.1% DM at 23 °C. Then 1 mM ferricyanide was added to ensure the oxidized state of CcO. Five minutes after initiation of the incubation, this sample was passed through a 2 cm × 25 cm Sephadex G25 column to remove all free reagents. The concentration of CcO·CN was calculated from the optical spectra using an extinction coefficient A_{428} of 163 mM^{-1} cm^{-1} for CcO·CN.[43]

Phospholipid Extraction. Lipids were extracted from CcO following the published protocol.[44] One milliliter of 35 *μ*M CcO [200 mM KP_i, 30 mM K_2SO_4 (pH 7.0), and 0.1% DM] was mixed thoroughly with 3 mL of a 2:1 (v/v) chloroform/methanol mixture, followed by centrifugation at 1000*g* for 10 min to separate the two phases. Most of the upper layer was removed by suction, and 2 mL of the lower chloroform layer was recovered by syringe. The chloroform layer was dried at 23 °C under a stream of N_2, and the lipid residue was dissolved in 2 mL of cyclohexane for optical absorption measurements. Lipid extraction was applied to two CcO samples. Both were exposed to 1 mM H_2O_2 for 30 min at 23 °C, the difference being that one sample was the complex with cyanide (2 mM NaCN in buffer) while the other was the uninhibited oxidized enzyme.

Determination of the Concentration and Rate of Decomposition of H_2O_2. The concentration of stock solutions of H_2O_2 was assessed from absorption measurements at 240 nm using an A_{240} of 40 M^{-1} cm^{-1}.[45] To detect changes in the concentration of H_2O_2 during the reaction with CcO, a fluorescent method using scopoletin and horseradish peroxidase (HRP) was employed.[46] The basis of this method is that the fluorescent scopoletin is oxidized to the nonfluorescent derivative by HRP in the presence of H_2O_2. The detection of H_2O_2 was performed in 50 mM potassium phosphate buffer (pH 7.0) containing 0.45 *μ*M HRP and 11 *μ*M scopoletin. Using these concentrations of HRP and scopoletin in the assays, fluorescence quenching was achieved in the time of manual mixing. To determine the kinetics of peroxide decomposition, small aliquots were taken from the reaction mixture at selected times of incubation and injected into the assay solution. The fluorescence measurements were conducted in a Cary Eclipse Spectrometer using excitation at 360 nm and the detection of emission at 460 nm.

dx.doi.org/10.1021/bi401078b | *Biochemistry* 2014, 53, 3564−3575

The kinetics of H_2O_2 degradation was measured in the presence of the native uninhibited CcO, CcO·CN with no free cyanide in the solution, and also in the buffer alone (Figure 1A). Because the contribution to the rate of H_2O_2 decomposition by CcO·CN is small and <13% of the values observed for CcO (Figure 1A), the determined rate constants were used without a correction (Figure 2A).

Steady-State Concentrations of Ferryl Intermediates. The concentrations of the two oxoferryl intermediates, **P** and **F**, generated in the reaction of CcO with H_2O_2, were obtained from the difference optical spectra of treated oxidase minus oxidized enzyme using the an $A_{607-630}$ of 11 mM^{-1} cm^{-1} for **P** and an $A_{580-630}$ of 5.3 mM^{-1} cm^{-1} for **F**.[47] For these (steady-state) measurements, the buffer with a pH of 8.0 (200 mM KP_i and 0.1% DM at 23 °C) was used.

Detection of Superoxide. The dye nitro blue tetrazolium (NBT) in molar excess over CcO was utilized to monitor the production of superoxide radical during the reaction of CcO with H_2O_2.[48] The reduction of NBT by superoxide generates the monoformazan (MF^+) whose concentration was assessed by the changes in the optical absorption spectrum. The concentration of NBT was quantified from the optical spectra using an extinction coefficient A_{257} of 61 mM^{-1} cm^{-1}.[48]

To determine the extinction coefficient of MF^+ under the specific conditions of the measurements, we have prepared MF^+ in ethanol by the reduction of 200 μM NBT with 100 μM sodium ascorbate. The addition of the substoichiometric amount of ascorbate resulted in the formation of 100 μM MF^+ in ethanol.[49] Then the known amount of MF^+ was transferred from ethanol into a buffer [200 mM KP_i (pH 7.0) containing either 0.1% Triton X-100 or 0.075% Tween 20]. From the optical spectrum of these samples (5% ethanol), we obtained an extinction coefficient $A_{517-700}$ of 17.2 ± 0.5 mM^{-1} cm^{-1} for MF^+. The quantification of superoxide formation was based on the stoichiometry of 2 mol of superoxide producing 1 mol of MF^+.

Determination of Oxygen Release. A model 53 oxygen monitor from Yellow Springs Instruments equipped with a Thermolyn type 7200 electrode and stirrer was used for the detection of O_2 release in the reaction of oxidized CcO with H_2O_2.

EPR Measurements. For assessment of a free radical produced in the reaction of CcO with H_2O_2, we employed the spin trapping technique. To the sample of 5 μM CcO and 110 mM spin trap POBN [α-(4-pyridyl-1-oxide)-*N*-*tert*-butylnitrone] was added 200 μM H_2O_2 [200 mM KP_i (pH 7.0) and 0.1% DM at 23 °C]. Immediately after the addition of peroxide, the sample was loaded into the glass capillary, and over a period of 20 min, the five EPR spectra were recorded. The Varian E-6 EPR spectrometer was used for the measurements with the following settings: frequency of 9.225 GHz, modulation amplitude of 2 G, modulation frequency of 100 kHz, scan time of 4 min, power of 20 mW, and temperature of 23 °C.

Rapid Kinetic Measurements. Two methods were employed in these measurements: the stopped-flow technique for the measurements of the reduction kinetics of heme *a* and heme a_3 and the flow-flash method to assess the reaction of the fully reduced enzyme with oxygen.

The kinetics of anaerobic reduction of CcO was measured in the rapid scanning OLIS RSM-1000 stopped-flow apparatus equipped with a 20 mm path length observation cell. The reduction of heme *a* by ferrocytochrome *c* was initiated by mixing in a 1:1 volume ratio of 3.7 μM CcO·CN with an anaerobic solution of 13.8 μM cytochrome *c* and 10 mM dithionite. In the CcO·CN complex, the transfer of the electron to heme a_3 is blocked by the ligand. This permits the selective measurement of the reduction kinetics of heme *a*. The kinetics of the reduction of heme *a* for two CcO·CN complexes were compared: the first complex was prepared from the enzyme as purified (native CcO), and the second was prepared from CcO after the treatment with 100 μM H_2O_2 for 3 h at 23 °C [10 mM Tris (pH 7.6) and 0.1% DM].

The internal ET from heme *a* to heme a_3 was measured under anaerobic conditions at pH 9.0. In this case, an anaerobic solution of 3.7 μM CcO was mixed with buffer [200 mM Ches (pH 9.0), 100 mM NaCl, and 0.1% DM] containing 10 mM Ru(II) and 10 mM sodium dithionite. A high concentration of Ru(II) was employed to reduce both Cu_A and heme *a* in the dead time of the stopped-flow instrument. The subsequent reduction of heme a_3 takes place on a time scale that can be recorded by this apparatus. The reduction of heme a_3 was recorded as changes in absorbance at 444 nm.

The flow-flash method was employed for monitoring the kinetics of oxidation of the fully reduced CcO with O_2. For these measurements, the preformed complex of 33.1 μM fully reduced CcO with carbon monoxide ($Cu_A^+Fe_a^{2+}Fe_{a3}^{2+}$-CO Cu_B^+) was rapidly mixed in a 1:1 volume ratio with oxygen-saturated buffer [1.25 mM O_2, 200 mM KP_i (pH 7.0), and 0.1% DM at 20 °C] into the observation cell (2 mm path length). Then the reaction with O_2 was triggered by photolyzing CO with a laser pulse (577 nm, 0.5 μs, phase-R 2100 dye laser), and the kinetics of oxidation of CcO was recorded at 445 nm. The rapid mixing of the solutions was achieved in a Bio-Logic stopped-flow module (SFM 400).

To prepare the complex of the fully reduced CcO with CO, the air in the sample of the oxidized enzyme was exchanged with argon. Then 0.5 μM cytochrome *c* and 25.5 mM ascorbic acid were added from a side arm of the tonometer to fully reduce the enzyme. To ensure complete reduction, the enzyme was incubated under 1.3 atm of CO for 20 min at 20 °C prior to beginning the kinetic measurements.

RESULTS

H_2O_2 Decomposition and Superoxide Production. In the absence of external electron donors, CcO is able to decompose hydrogen peroxide by turnover (Figure 1A, CcO). The kinetics of this decomposition was measured in the range between 50 and 800 μM H_2O_2 using 3 μM CcO (Figure 1B). A plot of the initial rate of decomposition versus peroxide concentration appears to exhibit hyperbolic behavior (Figure 2A). When this dependence was fit to the Michaelis–Menten equation, the following parameters were derived: k_{cat} = 0.07 s^{-1} (V_{max} = 0.2 μM s^{-1}), K_M = 230 μM, and $k_{cat}/K_M \approx 300$ M^{-1} s^{-1}. The apparent bimolecular rate constants of 200 M^{-1} s^{-1}[130] and 63 M^{-1} s^{-1}[139] were recently determined for the consumption of H_2O_2 by the bovine CcO purified by different protocols. We also observed that the increase in the CcO concentration leads to a proportional increase in the kinetics of H_2O_2 degradation. For example, increasing the concentration of CcO 2-fold, from 3 to 6 μM, increases the pseudo-first-order rate constant for the decomposition of 100 μM H_2O_2 from 6 × 10^{-4} to 1.1 × 10^{-3} s^{-1}. This rate was not substantially affected by changing the detergent in solution. The rate constants of 2 × 10^{-4} and 3.2 × 10^{-4} s^{-1} for the degradation of 100 μM H_2O_2 by 3 μM CcO were found in the buffer containing 0.1% Triton X-100 and 0.075% Tween 20, respectively.

dx.doi.org/10.1021/bi401078b | *Biochemistry* 2014, 53, 3564–3575

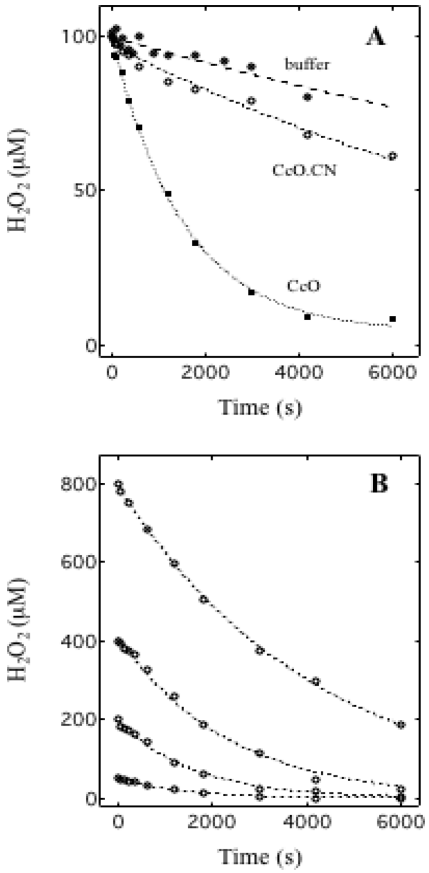

Figure 1. Kinetics of decomposition of H_2O_2 by oxidized cytochrome *c* oxidase. (A) Consumption of H_2O_2 by the oxidized enzyme (CcO), the enzyme in which the heme a_3−Cu_B center is blocked by cyanide (CcO.CN), and the enzyme in buffer without CcO (buffer). (B) Kinetics of decomposition of H_2O_2 by CcO at 50, 200, 400, and 800 μM peroxide. The dashed lines are monoexponential fits to the data. Conditions of measurements: 3.0 μM CcO in 200 mM potassium phosphate buffer (pH 7.0), 10 mM EDTA, and 0.1% DM at 23 °C.

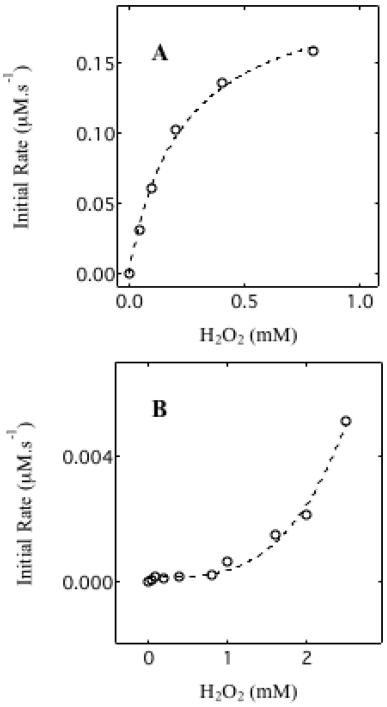

Figure 2. Kinetic dissimilarity between the decomposition of H_2O_2 and superoxide formation by cytochrome *c* oxidase. (A) Dependence of the initial rates of H_2O_2 decomposition on peroxide concentration. The dashed line is a fit of the data to the Michaelis−Menten equation. (B) Dependence of the initial rate of superoxide generation by CcO on the concentration of H_2O_2. The dotted line is a guideline enhancing the visualization of the dependence. Conditions of measurement were the same as those described in the legend of Figure 1, except that for superoxide detection 147 μM NBT was present in the buffer. The kinetics of formation of superoxide was monitored by changes in the absorbance difference of NBT at 517−700 nm.

Blocking the catalytic heme a_3−Cu_B center with cyanide significantly decreases the rate of H_2O_2 decomposition (Figure 1A, CcO.CN). The measurement using CcO·CN was performed in a buffer with no free cyanide. Very similar rates of H_2O_2 degradation were observed for the spontaneous decay of H_2O_2 in buffer only or in the presence of denaturated CcO (Figure 1A, buffer). These rates show that almost full inhibition of peroxide disintegration is accomplished by the exclusion of the heme a_3−Cu_B site from the process.

Previously, it had been suggested that degradation of H_2O_2 occurs via pseudocatalase activity at the heme a_3−Cu_B center. This activity should release the superoxide molecules whose dismutation is associated with O_2 formation.[30,34] We examined a possible oxygen release in the reaction of 3 μM oxidized CcO with 100 μM, 1 mM, and 5 mM H_2O_2. Under the given conditions [200 mM KP_i buffer and 10 mM EDTA (pH 7.0) at 23 °C], the production of O_2 was detected only at concentrations of 1 and 5 mM H_2O_2, while at 100 μM H_2O_2, oxygen formation was absent.

The measurement of the initial rates of superoxide generation, monitored by NBT, revealed two concentration regions with different characteristics for H_2O_2 decomposition (Figure 2B). Below ∼1 mM H_2O_2, there was almost no superoxide formation detected. However, above this concentration, superoxide production was observed. It appears that the peroxide concentration has to be above ∼1 mM to be able to produce superoxide in its reaction with CcO.

The spectral changes of NBT were completely suppressed by the addition of superoxide dismutase to the reaction buffer or by blocking the catalytic center of CcO with cyanide. Changing the concentration of NBT in the reaction to 300, 600, and 900 μM, the CcO concentration to 6 and 9 μM, the KP_i concentration from 200 to 20 mM, and the pH to 8 did not lead to the observation of superoxide formation when using a submillimolar concentration of H_2O_2. We have also verified that under our experimental conditions, the oxidation of preformed monoformazan cation (2 μM) by 3 μM CcO proceeds at a very slow rate (∼0.1 nM s^{-1}). This confirms that its oxidation cannot be responsible for the missing detection of superoxide.

In the millimolar range of peroxide concentrations, the initial rate of superoxide production appears to be linearly dependent on peroxide concentration up to 80 mM (not shown). The calculated bimolecular rate constant of 2.6 M^{-1} s^{-1} for superoxide generation from these data is in a good agreement with the published value of 2−4 M^{-1} s^{-1}.[35]

Transitions of CcO during Turnover. The overall transitions of CcO in the reaction with H_2O_2 were monitored via the time evolution of the UV−vis absorption spectrum of the enzyme (Figure 3). The difference spectra of CcO in the

dx.doi.org/10.1021/bi401078b | *Biochemistry* 2014, 53, 3564−3575

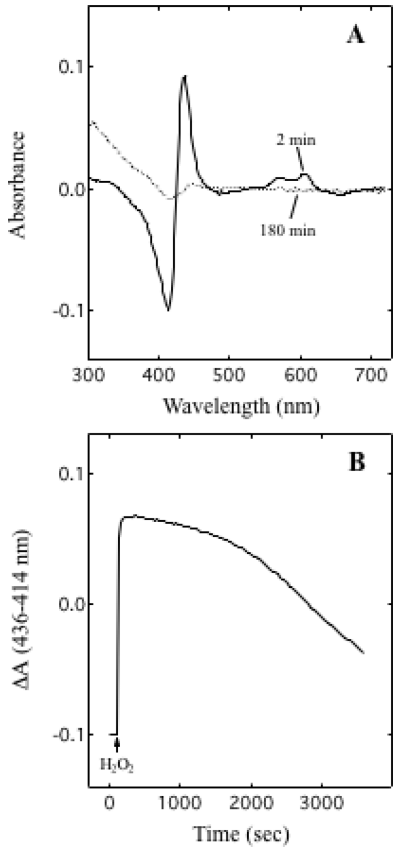

Figure 3. Spectral transitions of cytochrome *c* oxidase induced by H_2O_2. (A) Difference spectra of the peroxide-reacted CcO relative to that of the initial oxidized CcO. The spectra were recorded at 2 and 180 min following addition of 100 μM H_2O_2 to 3.5 μM CcO. (B) Time evolution of the absorbance changes [ΔA(436−414 nm)] of 3.5 μM CcO during the interaction with H_2O_2. At the time indicated by the arrow, 100 μM H_2O_2 was added. Conditions of the measurements were the same as those described in the legend of Figure 1.

presence of peroxide relative to that of the oxidized enzyme demonstrate the formation of the two ferryl intermediates, **P** and **F** (Figure 3A). Their presence can be distinguished in the α-band region where the peak at 607 nm indicates the **P** form and the maximum at 580 nm reflects the population of the enzyme in the **F** state (Figure 3A).

Because the Soret bands of **P** and **F** are almost identical,[27] the absorbance changes at 436−414 nm versus time do not discriminate between these two forms (Figure 3B). However, the kinetics of A(436−414 nm) shows (Figure 3B) that the steady state of the combined population of **P** and **F** is reached relatively quickly after the addition of excess peroxide. This steady state is followed by the disappearance of both oxoferryl forms with the subsequent recovery of the spectrum of the apparently oxidized CcO (Figure 3A).

In the transition from **P** and **F** to **O** (Figure 3B), some acceleration of the conversion is discernible at ∼1500 s. This increased rate of conversion is due to the limited availability of free H_2O_2. After this time point, the spontaneous decay of the ferryl states becomes the dominant reaction and their formation through the reaction of the recovered oxidized CcO with the residual free peroxide is substantially slower or even absent. Before this time, the peroxide concentration is high enough to maintain a sufficient rate of formation of **P** and **F** to compete with the decay rate of these intermediates to the oxidized enzyme.

It is known that the conversions of **O** to **P** and **P** to **F** are driven by H_2O_2.[22,24,25,29,50,51] Each of these steps is accomplished by 1 equiv of peroxide:[26,27]

$$\mathbf{O} + H_2O_2 \rightarrow \mathbf{P} + H_2O_2 \rightarrow \mathbf{F}$$

The third transition, from **F** to **O**, which has to occur during turnover, may be due to the reaction of **F** with an additional H_2O_2 molecule, may take place without the participation of peroxide by the endogenous decay of **F** to **O**, or is the result of the reduction of **F** with superoxide produced in the preceding **P** to **F** step. Which of these pathways dominates in the turnover can be evaluated from the dependence of the [**F**]/[**P**] molar ratio on the concentration of H_2O_2 under steady-state conditions. Using the steady-state approximation, it can be calculated that only in the case when the reaction cycle proceeds as $\mathbf{O} + H_2O_2 \rightarrow \mathbf{P} + H_2O_2 \rightarrow \mathbf{F} \rightarrow \mathbf{O}$, through the endogenous decay of $\mathbf{F} \rightarrow \mathbf{O}$, should the [**F**]/[**P**] ratio be linearly dependent upon peroxide concentration.

These measurements of the steady-state concentration of **P** and **F** were performed at pH 8.0 because the reaction of oxidized CcO with H_2O_2 is pH-dependent.[27,29,51] The major feature of this dependence is the branching of the reaction at the level of **P** that is under the control of an acid−base group(s) characterized for bovine heart oxidase with a pK_a of approximately 6.7−7.0.[25,29,52] Only at higher pH values, where the group is deprotonated, does the reaction of CcO with H_2O_2 proceed with the dominant production of **P**. Using excess H_2O_2, this initial **P** state is followed by the transition to **F** and consequently to the steady-state level characterized as a mixture of **P** and **F** (Figure 4A). Under these conditions, we found that the dependence of the steady-state [**F**]/[**P**] ratio on H_2O_2 concentration is linear (Figure 4B). This observation supports the model in which **O** is regenerated by the spontaneous or endogenous decomposition of **F**.

Decline of Catalytic Activity of CcO Treated with H_2O_2. The absence of almost any loss of the heme absorbance after peroxide treatment (Figure 3A) may imply the complete catalytic recovery of CcO. Despite this apparent spectral restoration, a substantial and irreversible decrease in the catalytic activity is observed for the H_2O_2-reacted CcO. Incubation of CcO with H_2O_2 initiates a progressive decline in its ability to oxidize ferrocytochrome *c* (Figure 5, H_2O_2). The activity decreases by ∼65% in a period of ∼3 h after incubation of CcO with 100 μM H_2O_2. This inactivation cannot be ascribed to the aging of the enzyme as the incubation of CcO in buffer alone under the same conditions causes a diminution of the activity by only ∼10% (Figure 5, buffer). The inactivation also takes place when CcO is not exposed to multiple turnovers with peroxide. This is the case when catalase is added to the sample immediately after all the CcO has reacted with H_2O_2 (Figure 5, H_2O_2/Cat). This simple endogenous decay of the intermediates to oxidized CcO diminishes the enzymatic activity by ∼40%.

Oxidation of CcO-Bound Lipids. In contrast to the reversibility of the absorbance of the heme centers, the exposure of CcO to peroxide produces an irreversible increase in the absorbance in the UV region. The kinetics of this process is illustrated in Figure 6A. However, the development of this absorbance takes place only if peroxide is present in the solution. Adding catalase to the sample during the reaction of CcO with H_2O_2 completely stops this increase in absorption

dx.doi.org/10.1021/bi401078b | *Biochemistry* 2014, 53, 3564−3575

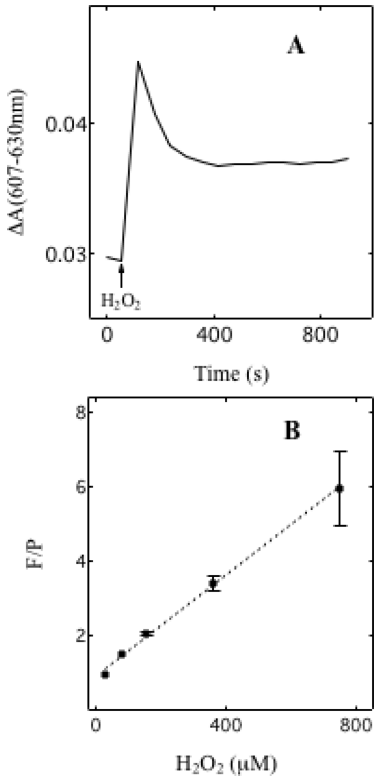

Figure 4. Dependence of the molar ratio of ferryl (**F**) to the peroxy (**P**) form on H_2O_2 concentration under steady-state conditions. (A) Kinetics of transitions of 3.0 μM oxidized CcO to the steady-state level of **P** induced by 200 μM H_2O_2. The transition is monitored as the spectral change at 607 nm. (B) Dependence of the steady-state [**F**]/[**P**] molar ratio on H_2O_2 concentration. The steady-state concentrations of **F** and **P** forms were determined from the difference spectra of 3.0 μM CcO exposed to peroxide vs oxidized enzyme. Measurements were performed in a solution of 200 mM KP_i (pH 8.0), 0.08% DM, and 5 mM diethylenediaminepentaacetic acid at 23 °C. The data points are the averages of three measurements, and for each measurement, a fresh sample of CcO was used. The dashed line is the linear fit.

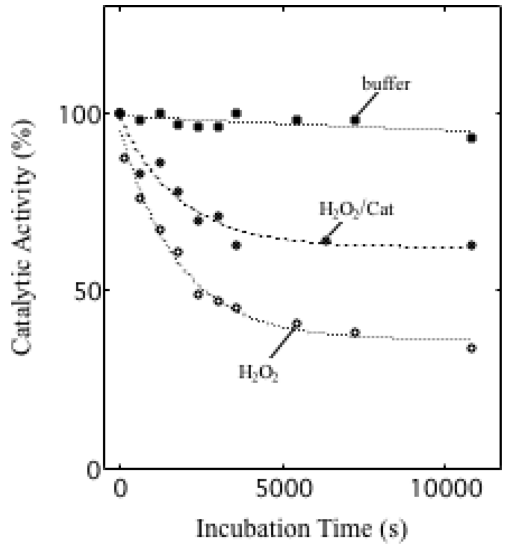

Figure 5. Decline of the catalytic activity of cytochrome *c* oxidase during incubation with H_2O_2. The catalytic activity of CcO during the reaction of 3.3 μM CcO with H_2O_2 was determined for (○) CcO incubated with 100 μM H_2O_2, (■) CcO reacted with 100 μM H_2O_2 for 120 s and then residual peroxide removed from solution by the addition of catalase (3000 units), and (●) CcO incubated in buffer only [200 mM potassium phosphate (pH 7.0) and 0.1% DM at 23 °C] in the absence of hydrogen peroxide. Aliquots of the enzyme were removed from the samples at selected times, and the catalytic activity was assessed by measuring the rate of the oxidation of 7 μM ferrocytochrome *c* by 15 nM CcO. The molecular activity is expressed as a percentage of the rate of the oxidation of ferrocytochrome *c* by the untreated oxidized CcO. The absolute value at time zero, expressed as the number of electrons transferred by CcO, corresponds to an activity of ~14 s^{-1}. The dashed lines are monoexponential fits to the data.

(Figure 6A). This spectral development was also absent when the catalytic heme a_3–Cu_B center was blocked by cyanide. In the presence of superoxide dismutase (SOD, 150 units/mL), the amplitude of this spectral change was slightly decreased (1–5%) relative to that of a control lacking SOD. Replacing the air with argon has no measurable effect on the development of this transition.

The difference spectrum in the UV region of the peroxide-reacted CcO versus untreated enzyme exhibits a positive band at ~274 nm together with a large increase in the absorbance below 250 nm (Figure 6B). The appearance of these bands is indicative of the formation of conjugated dienes and trienes[53−55] produced by the oxidation of the lipids copurified with CcO.[8,9,56] To verify this possibility, we examined the lipids extracted from two samples of CcO subjected to the reaction with H_2O_2. In the first sample, the enzyme was inhibited by cyanide while the second sample contained native, uninhibited CcO. The spectrum of the lipids from uninhibited CcO shows the substantial increase in the absorbance in the UV region relative to that of the lipids extracted from the cyanide-inhibited enzyme (Figure 6C, CcO.CN). The similarity of the absorbance changes in CcO and the extracted lipids shows that, indeed, the bound lipids are the sites of modification of the enzyme by peroxide.

Generation of Lipid-Derived Radical. In the course of the reaction of CcO with peroxide, we observed the production of organic free radical. The formation of the radical is demonstrated by the EPR spectrum of the spin trap POBN–radical adduct (Figure 7). The cumulative spectrum shows six lines characterized by the following hyperfine coupling constants: a^N = 16.1 G, and a^H = 2.7 G. Very similar coupling constants (a^N = 15.8 G, and a^H = 2.5–2.6 G) were attributed previously to either the carbon-centered radical of a POBN–linoleic acid adduct[57] or the adduct of POBN with a lipid peroxyl radical.[58] No EPR signals were detected in experiments in which CcO·CN was reacted with 200 μM H_2O_2.

Electron Transfer in Peroxide-Modified CcO. To identify the impaired step in the overall catalytic cycle of the peroxide-reacted CcO, we examined the kinetics of ET under three conditions. We have measured the kinetics of ET in both native and peroxide-treated CcO from ferrocytochrome *c* to heme *a* (Figure 8A) and from heme *a* to heme a_3 (Figure 8B) and the kinetics of oxidation of the fully reduced oxidase with O_2 (Figure 8C).

Nearly identical amplitudes and kinetics of the anaerobic reduction of heme *a* by ferrocytochrome *c* (Figure 8A) show that peroxide treatment does not affect the entry of an electron into CcO. The apparent rate constants obtained from the monoexponential fits of data for untreated and H_2O_2-treated CcO are 4 ± 0.2 and 3.9 ± 0.2 s^{-1}, respectively.

dx.doi.org/10.1021/bi401078b | *Biochemistry* 2014, 53, 3564–3575

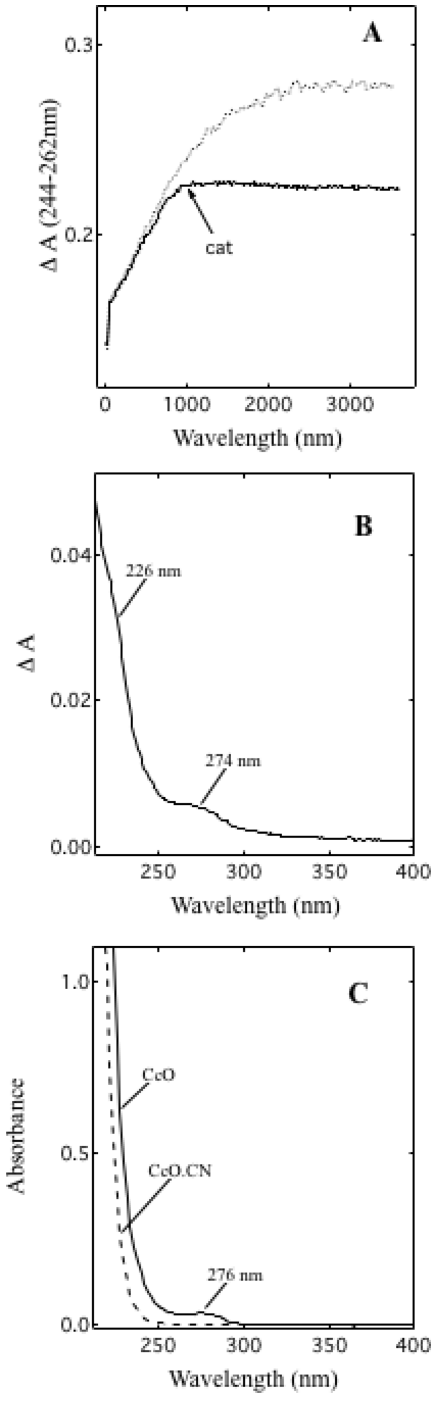

Figure 6. Spectral changes of cytochrome *c* oxidase and the protein-bound lipids induced by H_2O_2. (A) Development of the irreversible UV spectral change of CcO [ΔA(244−262 nm)] caused by H_2O_2 (···) and effect of catalase on the progress of these changes (—). The addition of catalase (3000 units/mL) is indicated by the arrow. In both samples, 3.0 μM CcO was reacted with 100 μM H_2O_2. The reaction with peroxide was initiated at time zero. Conditions of the measurements are the same as those described in the legend of Figure 1. (B) UV difference spectrum of 3 μM CcO monitored 3 h after the reaction with 100 μM H_2O_2 vs the initial oxidized CcO. The buffer consisted of 200 mM KP_i (pH 7.0) and 0.1% DM. (C) Spectrum of lipids extracted from CcO samples exposed to H_2O_2: (CcO) spectrum of lipids obtained from the uninhibited oxidase and (CcO.CN) spectrum of lipids from the oxidase in which the catalytic center was blocked by cyanide. The spectra were collected on the lipids dissolved in cyclohexane.

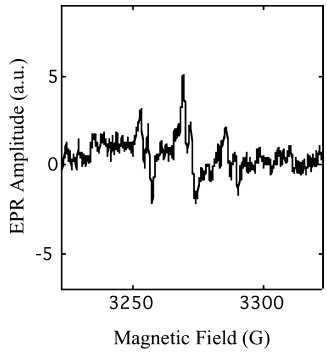

Figure 7. Generation of lipid-centered radical in the reaction of cytochrome *c* oxidase with H_2O_2. Cumulative spectrum of the POBN−radical adduct recorded on the sample in which 5.0 μM CcO reacted with 200 μM H_2O_2 for 20 min. The buffer consisted of 200 mM potassium phosphate (pH 7.0), 0.1% DM, and 110 mM POBN at 23 °C. For a detailed description of the measurements and conditions, see Experimental Procedures.

However, quite different kinetic behavior was observed for internal ET from heme *a* to a_3 (Figure 8B). The kinetics of the heme a_3 anaerobic reduction in the untreated enzyme was biphasic; the major phase, which contributed 88% to the absorbance change, is characterized by a rate constant of 13 ± 0.4 s^{-1}. The corresponding phase for heme a_3 reduction in H_2O_2-modified CcO contributes 70% to the absorbance change and proceeds with a rate constant of 4 ± 0.2 s^{-1}. This rate corresponds to one-third of that observed in the untreated enzyme. It is noted that the almost identical amplitudes of the absorbance change of heme a_3 observed for the native and peroxide-modified enzyme show that the same amount of heme a_3 is reduced in each form of the enzyme.

To measure the kinetics of oxidation of reduced CcO with O_2, the fully reduced CcO was prepared with carbon monoxide bound at the heme a_3−Cu_B center and the reaction with O_2 was initiated by photodissociation of the CO. The subsequent spectral changes take place in four kinetically distinguishable phases (Figure 8C). All phases and their assignment to particular intermediates were established in previous studies.[59−61] The immediate absorbance increase at 445 nm comes from the photodissociation of CO and the appearance of nonligated reduced heme a_3. The interaction of the uninhibited enzyme with O_2 results in a rapid decrease in the absorbance at 445 nm, and this phase ends with the formation of $\mathbf{P_R}$. The subsequent small absorbance increase represents the conversion of $\mathbf{P_R}$ to **F**. The transition of **F** to oxidized CcO is the final phase that occurs with a rate constant of 594 ± 43 s^{-1} for the untreated enzyme (Figure 8C, control) and 622 ± 44 s^{-1} for H_2O_2-treated CcO (Figure 8C, H_2O_2 treated). In spite of the complex kinetic pattern, a comparison of both kinetic traces shows that the transition of the fully reduced enzyme to oxidize CcO is not altered by the peroxide treatment.

Altogether, the kinetic measurements demonstrate that the peroxide treatment of CcO results in a quite specific impact on the internal electron transfer from heme *a* to a_3 (Figure 8B). The extent of this inhibition correlates well with the observed decrease in the overall catalytic activity of the enzyme (Figure 5).

DISCUSSION

Reduction of H_2O_2 at the Catalytic Center. The continuous reduction of H_2O_2 at the catalytic center of CcO

dx.doi.org/10.1021/bi401078b | *Biochemistry* 2014, 53, 3564−3575

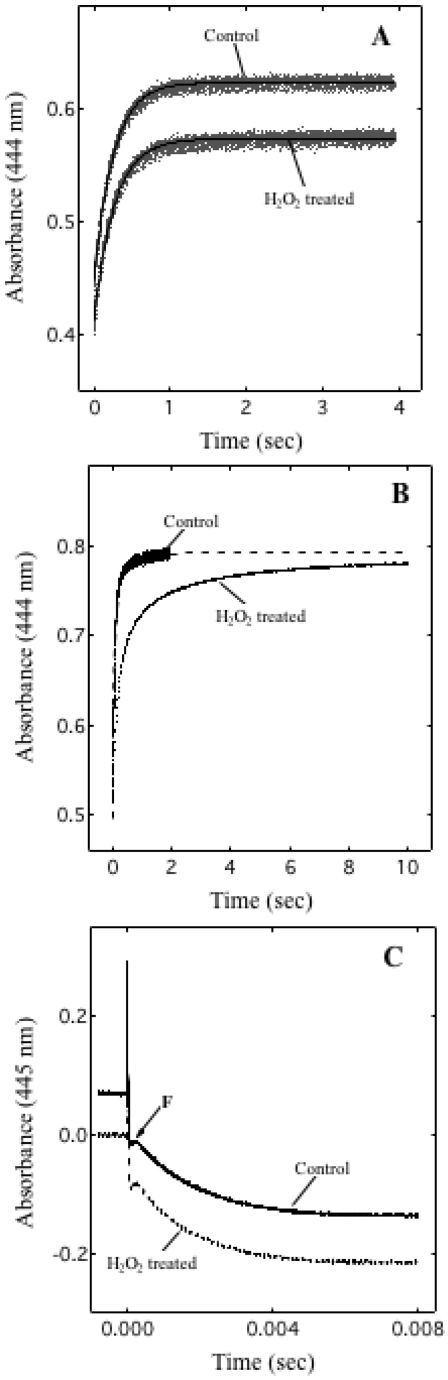

Figure 8. Effect of H_2O_2 modification of cytochrome *c* oxidase on the kinetics of electron transport. (A) Kinetics of transfer of an electron from ferrocytochrome *c* to heme *a* for both native (control) and peroxide-modified CcO (H_2O_2-treated). The catalytic center in both CcO samples was blocked by cyanide (10 mM), and the reduction kinetics was measured using 7.0 μM ferrocytochrome *c* and 5 mM sodium dithionite. The dots are the recorded traces and the solid lines the monoexponential fits to the data. The control trace is offset by +0.04 OD unit. (B) Kinetics of internal ET from heme *a* to heme a_3 for native (control) and peroxide-modified CcO (H_2O_2-treated). CcO is reduced by a mixture of 5 mM Ru(II) and 5 mM dithionite under anaerobic conditions. All measurements were performed with 1.8 μM CcO in 200 mM Ches buffer (pH 9.0), 100 mM NaCl, and 0.1% DM at 23 °C. Concentrations are after the mixing in the stopped-flow apparatus. Progress of the reduction of heme *a* and a_3 was monitored as a change in absorbance at 444 nm. The dashed line is an extension of the two-exponential fit of data up to 10 s. H_2O_2-treated enzyme was prepared via preincubation of CcO for 3 h with 100 μM H_2O_2 in 200 mM potassium phosphate buffer (pH 7.0) and 0.1% DM at 23 °C. (C) Kinetics of oxidation of fully reduced cytochrome oxidase with O_2. Anaerobic fully reduced native (control) and peroxide-treated CcO (H_2O_2-treated) complexed with carbon monoxide were mixed rapidly with oxygen-saturated buffer in the flow-flash apparatus. At time zero, the reaction with O_2 was initiated by photodissociation of CO by a laser pulse. The redox transitions from the reduced to oxidized enzyme were monitored as the change in absorbance at 445 nm. The traces mostly show the last phase of the reaction, the conversion of the accumulated ferryl intermediate (**F**) to the oxidized enzyme. The peroxide-treated enzyme was prepared by preincubation of 33.1 μM CcO with 600 μM H_2O_2 for 1 h at 23 °C. The trace of the untreated control is offset by +0.07 absorbance unit.

via the **P** and **F** intermediates has been previously attributed to the pseudocatalase function of the enzyme.[24,30,34,35] According to this proposal, free H_2O_2 acts as a one-electron donor for the transition of **P** to **F** or even for the conversion of **F** to **O**.[30] The two superoxide anions expected to be formed in transitions of **P** to **F** and **F** to **O** are released and subsequently dismute to peroxide and O_2.[30,34] We demonstrated that at a low H_2O_2 concentration (below ~1 mM) (Figure 4), only two molecules of peroxide are involved in the single turnover of CcO, utilizing the pathway

$$\mathbf{O} + H_2O_2 \rightarrow \mathbf{P} + H_2O_2 \rightarrow \mathbf{F} \rightarrow \mathbf{O}$$

where the first H_2O_2 produces **P** from **O** and the second converts **P** to **F**. This process is followed by the endogenous decay of **F** to **O**. However, the absence of both superoxide (Figure 2B) and oxygen release during the cycle shows that the pseudocatalase mechanism is not in effect or has only a very weak contribution in the submillimolar H_2O_2 concentration range. Consequently, it raises the question about the nature of the reactions in this cycle.

Previous investigations showed that the reaction of **O** with H_2O_2 is the redox reaction producing both the oxoferryl heme iron and a putative radical ($Y^\bullet$) in the vicinity of the heme a_3–Cu_B center in the **P** state.[15,62−65] The nature of the second reaction, the conversion of **P** to **F**, is enigmatic and very interesting. This transition, without the formation of superoxide, can be accomplished by two different mechanisms (Figure 9). The first is that the **P** to **F** transition results from a structural rearrangement of CcO.[66] We assume, in accord with an earlier suggestion,[23] that the binding of the second molecule of H_2O_2 to Cu_B triggers a structural change. This explanation has some support in the observed conversion of $\mathbf{P_R}$ to the **F** intermediate during the reaction of fully reduced CcO with O_2. The oxoferryl $\mathbf{P_R}$ state, spectrally very similar if not identical to the **P** intermediate[17] (but see ref 67), is formed after three electrons are delivered to the catalytic center in the reaction with O_2. It is presumed that the neutral radical $Y^\bullet$ present in **P** (Fe_{a3}^{IV}=O Cu_B^{II} $Y^\bullet$) is annihilated in the $\mathbf{P_R}$ intermediate (Fe_{a3}^{IV}=O Cu_B^{II} Y). The spectral conversion of $\mathbf{P_R}$ to **F** is associated with the proton uptake and release without any electron transfer to the catalytic center.[68−71] The second possibility for **P** to **F** conversion is the redox reaction (Figure 9). According to this proposition, H_2O_2 is cleaved at Cu_B into two $HO^\bullet$ radicals and one of these radicals annihilates $Y^\bullet$. The second $HO^\bullet$ radical propagates the oxidative damage of the enzyme.

dx.doi.org/10.1021/bi401078b | *Biochemistry* 2014, 53, 3564−3575

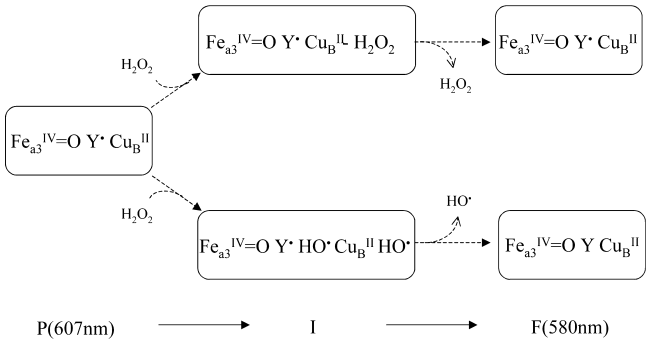

Figure 9. Proposed pathways for the conversion of P to F stimulated by H_2O_2. Two reactions responsible for the **P**(607 nm) to **F**(580 nm) transition triggered by H_2O_2 proceed through the intermediate state (**I**). In **P**, the iron of heme a_3 is in the oxyferryl state, and it is expected that at the catalytic heme a_3−Cu_B center (oval box) the radical (Tyr244, Y•) is also present. The ligation state of Cu_B is excluded from consideration. The top path represents the conversion stimulated by the peroxide binding to Cu_B. The transition is associated with the change in affinity of Cu_B for H_2O_2 that is followed by the dissociation of peroxide. In the bottom path, one of the two hydroxyl radicals, produced by homolytic splitting of H_2O_2, is able to annihilate the Y• radical. The second HO• radical is released from the catalytic center. The presence or absence of the neutral Y• radical in the **F** form is presumed to not affect in a substantial way the optical absorption spectra of heme a_3.

Our data indicate that two molecules of H_2O_2 participate in the formation of **F** from the oxidized enzyme. However, in the recovery of **O** from **F**, peroxide or superoxide is not involved. This implies that the oxoferryl state of iron of heme a_3 is reduced to ferric iron by the endogenous oxidation of the protein and lipid components of purified CcO. This autoxidation is accompanied by the progressive loss of the catalytic activity of the enzyme during the conversion of **F** to **O** (Figure 5).

The described cycle of peroxide reduction at the catalytic center is, however, restricted to H_2O_2 concentrations below ∼1 mM. In this submillimolar range, the action of CcO is characterized by the absence of the production of both superoxide (Figure 2B) and O_2 from peroxide. In contrast, the reactions of CcO with peroxide above 1 mM H_2O_2 result in the release of both O_2 and superoxide. This change in product formation indicates that with increasing H_2O_2 concentrations there is a gradual change in the mechanism of peroxide decomposition by CcO. One is effective in the submillimolar range, and the second prevails at millimolar H_2O_2 concentrations.

This conclusion is also supported by the different rates of peroxide decomposition and superoxide production by CcO at submillimolar and millimolar H_2O_2 concentrations. The dependence of the rate of peroxide decomposition on H_2O_2 concentration conforms to the Michaelis−Menten approximation below 1 mM H_2O_2 (Figure 2A). This dependence suggests that the rate of peroxide decomposition should approach a limiting value at ∼1 mM H_2O_2. However, this observation contradicts the observation that superoxide generation increases linearly with the increase in peroxide concentration from 2 to 80 mM H_2O_2. This discrepancy is an additional fact in favor of the change in the mechanism of peroxide decomposition by CcO caused by the increased concentration of H_2O_2.

Secondary Sites of H_2O_2 Decomposition. A discrepancy between the rates of **P** and **F** production and the rates of superoxide production and peroxide consumption using the linear sequential model has already been noted.[30,35] This kinetic mismatch can be reconciled by the presence of the additional reaction(s) of peroxide with CcO that is not confined to the heme a_3−Cu_B center. These secondary reactions are indicated by two observations. The first is the generation of the surface-exposed lipid-based radical (Figure 7) that is initiated by the reaction of H_2O_2 with the catalytic center. Protein-based radicals like thiyl and tyrosine[72] and hydroxyl radicals[72] were already observed under similar experimental conditions that we have utilized in this study. Additionally, we have established the reaction between the protein-bound lipids and the free peroxide in solution (Figure 6). Similar to radical formation, this reaction is also fueled by the initial interaction of H_2O_2 with the catalytic center. On the basis of these two observations, we suggest that the lipid-based radicals and possibly protein radicals react with the free peroxide, leading to the peroxidation of CcO-bound lipids and the promotion of the oxidative damage of these distant sites of the enzyme.

The proposed radical pathway can explain the degradation of the vast molar excess of peroxide by a low concentration of the enzyme (Figure 1). The surface-exposed radical (R•) can decompose peroxide to water by the self-propagating chain reactions

$$R^\bullet + H_2O_2 \rightarrow R\text{-}OH + HO^\bullet$$

$$R\text{-}H + HO^\bullet \rightarrow R^\bullet + H_2O$$

This reaction will continue as long as the active radical is not quenched by a second radical.

The appearance of radicals on the surface of the enzyme, formation of which is triggered by the reaction of H_2O_2 with the heme a_3−Cu_B center, can be explained by two different reactions. The first, previously suggested,[37,38] is the production of R• by the intraprotein electron transfer from surface sites to both the highly oxidative oxoferryl state and the putative radical (Y•) at or near the catalytic center. The second route for generation of R• is based on formation of HO• radicals during the **P** to **F** conversion (Figure 9). If these hydroxyl radicals can reach the surface of the enzyme, they could react with the bound lipids as well with some other distant groups.

All our measurements were performed on the solubilized enzyme in the presence of 0.1% detergent (dodecyl maltoside). Thus, we can expect that organic groups, functioning as electron donors, will not come exclusively from the proteolipid CcO complex. It is likely that R• can additionally be produced from the detergent. Because the concentration of the detergent is sufficiently high, its oxidation may sustain the degradation of excess peroxide. Moreover, an additional contribution to peroxide degradation is suggested by the study of the peroxidase activity of CcO. As shown previously, CcO exhibits peroxidase activity with organic compounds usually considered to be redox inactive.[73] Then it is conceivable that some product(s) of the oxidatively modified detergent may serve as the true electron donor for CcO, and this reaction will contribute to the reduction of H_2O_2 at the heme a_3−Cu_B center.

Selective Inhibition of Catalytic Activity. The reactions of oxidized CcO and H_2O_2 always result in a decrease in the catalytic activity of the enzyme (Figure 5). The time of incubation and the concentrations of peroxide employed, which

dx.doi.org/10.1021/bi401078b | *Biochemistry* 2014, 53, 3564−3575

determine the number of cycles at the heme a_3−Cu_B center, progressively increase the extent of damage to CcO. This progressive decline in catalytic activity can be understood by the accumulation of the damaged sites in CcO (Figure 5).[37] Obviously, the multiplication of the modified amino acid residues[37,38] and/or bound phospholipids is the most plausible reason for the loss of activity.[40,74,75]

Interestingly, we found that the loss of the catalytic activity of the peroxide-treated CcO was only associated with the diminution of the rate of ET from heme *a* to the catalytic heme a_3 center during the reductive phase of the catalytic cycle (Figure 8B). There are at least three events that may control ET during the anaerobic reduction of the heme a_3−Cu_B center in native CcO. The first is an apparent uptake of two protons[42,76] through the K-channel[77,78] that coincides with the reduction of the heme a_3−Cu_B center.[79] The second is the release of the native bridging ligand between oxidized Fe_{a3}^{3+} and Cu_B^{2+},[11,80−82] associated with reduction. The third is a structural change at the catalytic center demonstrated by the increase in the distance between Fe_{a3}^{2+} and Cu_B^{+} relative to that in the oxidized state.[8,82] At present, there are no structural data or data on proton uptake or ligand release available for peroxide-treated CcO. However, we can assume that the reduction of the peroxide-modified enzyme is also associated with corresponding events that may control the rate of ET. Consequently, the modification of any of these processes may have an adverse effect on ET.

One simple explanation for the specific inhibition of ET between hemes *a* and a_3 in the reductive phase of the catalytic cycle is an impairment of the K-channel produced by peroxide treatment. In this view, ET to the heme a_3−Cu_B center is inhibited because of the impaired delivery of a proton to the catalytic site via the modified K-channel.[77,78] This selective impairment of the K-channel without modification of the D-channel is consistent with the kinetics of **F** to **O** conversion during the reaction of fully reduced CcO with O_2 (Figure 8C). The **F** to **O** transition is controlled by the delivery of a proton through the D-channel, and the absence of any effect of peroxide on this reaction indicates that this channel is intact.[83,84]

AUTHOR INFORMATION

Corresponding Authors

*Department of Biophysics, University of P. J. Safarik, Jesenna 5, 041 54 Kosice, Slovak Republic. E-mail: daniel.jancura@upjs.sk. Phone: ++421 552342246. Fax: ++421 556222124.

*Rice University, 6100 Main St., MS 140, Houston, TX 77005. E-mail: fabian@rice.edu. Phone: (713) 348-2373. Fax: (713) 348-5365.

Funding

This work was supported by National Institutes of Health Grants GM 084348 (M.F.) and GM 080575 (G.P.) and FP7 EU Project CELIM 316310.

Notes

The authors declare no competing financial interest.

ACKNOWLEDGMENTS

We are grateful to Drs. R. J. Kulmacz and G. Wu for access to and instructions about the use of the oxygen monitor.

DEDICATION

Dedicated to the memory of Professor Vladimir Hajko, inspirational mentor and dear colleague.

ABBREVIATIONS

CcO, cytochrome *c* oxidase; CcO·CN, cytochrome *c* oxidase with cyanide bound at the heme a_3−Cu_B center; Fe_a, iron of heme *a*; Fe_{a3}, iron of heme a_3; Cu_A, dinuclear copper center; Cu_B, copper at the catalytic site; ET, electron transport; DM, *n*-dodecyl *β*-D-maltoside; SOD, superoxide dismutase; NBT, nitro blue tetrazolium; HRP, horseradish peroxidase; DEPA, diethylenediaminepentaacetic acid; POBN, *α*-(4-pyridyl-1-oxide)-*N*-*tert*-butylnitrone.

REFERENCES

(1) Wikstrom, M. (2012) Active site intermediates in the reduction of O_2 by cytochrome oxidase, and their derivatives. *Biochim. Biophys. Acta 1817*, 468−475.

(2) Siletsky, S. A., and Konstantinov, A. A. (2012) Cytochrome c oxidase: Charge translocation coupled to single-electron partial steps of the catalytic cycle. *Biochim. Biophys. Acta 1817*, 476−488.

(3) Ferguson-Miller, S., Hiser, C., and Liu, J. (2012) Gating and regulation of the cytochrome c oxidase proton pump. *Biochim. Biophys. Acta 1817*, 489−494.

(4) Capitanio, N., Palese, L. L., Capitanio, G., Martino, P. L., Richter, O. M., Ludwig, B., and Papa, S. (2012) Allosteric interactions and proton conducting pathways in proton pumping *aa*(3) oxidases: Heme *a* as a key coupling element. *Biochim. Biophys. Acta 1817*, 558−566.

(5) Konstantinov, A. A. (2012) Cytochrome c oxidase: Intermediates of the catalytic cycle and their energy-coupled interconversion. *FEBS Lett. 586*, 630−639.

(6) Kadenbach, B., Jarausch, J., Hartmann, R., and Merle, P. (1983) Separation of mammalian cytochrome c oxidase into 13 polypeptides by a sodium dodecyl sulfate-gel electrophoretic procedure. *Anal. Biochem. 129*, 517−521.

(7) Iwata, S., Ostermeier, C., Ludwig, B., and Michel, H. (1995) Structure at 2.8 Å resolution of cytochrome c oxidase from *Paracoccus denitrificans*. *Nature 376*, 660−669.

(8) Tsukihara, T., Aoyama, H., Yamashita, E., Tomizaki, T., Yamaguchi, H., Shinzawa-Itoh, K., Nakashima, R., Yaono, R., and Yoshikawa, S. (1996) The whole structure of the 13-subunit oxidized cytochrome c oxidase at 2.8 Å. *Science 272*, 1136−1144.

(9) Robinson, N. C., Strey, F., and Talbert, L. (1980) Investigation of the essential boundary layer phospholipids of cytochrome c oxidase using Triton X-100 delipidation. *Biochemistry 19*, 3656−3661.

(10) Robinson, N. C. (1982) Specificity and binding affinity of phospholipids to the high-affinity cardiolipin sites of beef heart cytochrome c oxidase. *Biochemistry 21*, 184−188.

(11) Qin, L., Hiser, C., Mulichak, A., Garavito, R. M., and Ferguson-Miller, S. (2006) Identification of conserved lipid/detergent-binding sites in a high-resolution structure of the membrane protein cytochrome c oxidase. *Proc. Natl. Acad. Sci. U.S.A. 103*, 16117−16122.

(12) Shinzawa-Itoh, K., Aoyama, H., Muramoto, K., Terada, H., Kurauchi, T., Tadehara, Y., Yamasaki, A., Sugimura, T., Kurono, S., Tsujimoto, K., Mizushima, T., Yamashita, E., Tsukihara, T., and Yoshikawa, S. (2007) Structures and physiological roles of 13 integral lipids of bovine heart cytochrome c oxidase. *EMBO J. 26*, 1713−1725.

(13) Proshlyakov, D. A., Pressler, M. A., and Babcock, G. T. (1998) Dioxygen activation and bond cleavage by mixed-valence cytochrome c oxidase. *Proc. Natl. Acad. Sci. U.S.A. 95*, 8020−8025.

(14) Fabian, M., Wong, W. W., Gennis, R. B., and Palmer, G. (1999) Mass spectrometric determination of dioxygen bond splitting in the "peroxy" intermediate of cytochrome c oxidase. *Proc. Natl. Acad. Sci. U.S.A. 96*, 13114−13117.

(15) Proshlyakov, D. A., Pressler, M. A., DeMaso, C., Leykam, J. F., DeWitt, D. L., and Babcock, G. T. (2000) Oxygen activation and

reduction in respiration: Involvement of redox-active tyrosine 244. *Science 290*, 1588−1591.
(16) Gorbikova, E. A., Belevich, I., Wikstrom, M., and Verkhovsky, M. I. (2008) The proton donor for O-O bond scission by cytochrome c oxidase. *Proc. Natl. Acad. Sci. U.S.A. 105*, 10733−10737.
(17) Morgan, J. E., Verkhovsky, M. I., Palmer, G., and Wikstrom, M. (2001) Role of the P_R intermediate in the reaction of cytochrome c oxidase with O_2. *Biochemistry 40*, 6882−6892.
(18) Han, S., Ching, Y. C., and Rousseau, D. L. (1990) Ferryl and hydroxy intermediates in the reaction of oxygen with reduced cytochrome c oxidase. *Nature 348*, 89−90.
(19) Varotsis, C., and Babcock, G. T. (1990) Appearance of the ν(Fe(IV)═O) vibration from a ferryl-oxo intermediate in the cytochrome oxidase/dioxygen reaction. *Biochemistry 29*, 7357−7362.
(20) Kitagawa, T., and Ogura, T. (1997) Oxygen activation mechanism at the binuclear site of heme-copper oxidase superfamily as revealed by time-resolved resonance Raman spectroscopy. *Prog. Inorg. Chem. 45*, 431−479.
(21) Einarsdottir, O., and Szundi, I. (2004) Time-resolved optical absorption studies of cytochrome oxidase dynamics. *Biochim. Biophys. Acta 1655*, 263−273.
(22) Wrigglesworth, J. M. (1984) Formation and reduction of a 'peroxy' intermediate of cytochrome c oxidase by hydrogen peroxide. *Biochem. J. 217*, 715−719.
(23) Vygodina, T., and Konstantinov, A. A. (1987) Evidence for two H_2O_2-binding sites in ferric cytochrome c oxidase. Indication to the O-cycle? *FEBS Lett. 219*, 387−392.
(24) Vygodina, T. V., and Konstantinov, A. A. (1988) H_2O_2-induced conversion of cytochrome c oxidase peroxy complex to oxoferryl state. *Ann. N.Y. Acad. Sci. 550*, 124−138.
(25) Vygodina, T., and Konstantinov, A. (1989) Effect of pH on the spectrum of cytochrome c oxidase hydrogen peroxide complex. *Biochim. Biophys. Acta 973*, 390−398.
(26) Weng, L. C., and Baker, G. M. (1991) Reaction of hydrogen peroxide with the rapid form of resting cytochrome oxidase. *Biochemistry 30*, 5727−5733.
(27) Fabian, M., and Palmer, G. (1995) The interaction of cytochrome oxidase with hydrogen peroxide: The relationship of compounds P and F. *Biochemistry 34*, 13802−13810.
(28) Brittain, T., Little, R. H., Greenwood, C., and Watmough, N. J. (1996) The reaction of *Escherichia coli* cytochrome bo with H_2O_2: Evidence for the formation of an oxyferryl species by two distinct routes. *FEBS Lett. 399*, 21−25.
(29) Junemann, S., Heathcote, P., and Rich, P. R. (2000) The reactions of hydrogen peroxide with bovine cytochrome c oxidase. *Biochim. Biophys. Acta 1456*, 56−66.
(30) Bolshakov, I. A., Vygodina, T. V., Gennis, R., Karyakin, A. A., and Konstantinov, A. A. (2010) Catalase activity of cytochrome c oxidase assayed with hydrogen peroxide-sensitive electrode microsensor. *Biochemistry (Moscow) 75*, 1352−1360.
(31) Gorren, A. C., Dekker, H., and Wever, R. (1985) The oxidation of cytochrome c oxidase by hydrogen peroxide. *Biochim. Biophys. Acta 809*, 90−96.
(32) von der Hocht, I., van Wonderen, J. H., Hilbers, F., Angerer, H., MacMillan, F., and Michel, H. (2011) Interconversions of P and F intermediates of cytochrome c oxidase from *Paracoccus denitrificans*. *Proc. Natl. Acad. Sci. U.S.A. 108*, 3964−3969.
(33) Hilbers, F., von der Hocht, I., Ludwig, B., and Michel, H. (2013) True wild type and recombinant wild type cytochrome c oxidase from *Paracoccus denitrificans* show a 20-fold difference in their catalase activity. *Biochim. Biophys. Acta 1827*, 319−327.
(34) Ksenzenko, M., Vygodina, T. V., Berka, V., Ruuge, E. K., and Konstantinov, A. A. (1992) Cytochrome oxidase-catalyzed superoxide generation from hydrogen peroxide. *FEBS Lett. 297*, 63−66.
(35) Konstantinov, A. A., Capitanio, N., Vygodina, T. V., and Papa, S. (1992) pH changes associated with cytochrome c oxidase reaction with H_2O_2: Protonation state of the peroxy and oxoferryl intermediates. *FEBS Lett. 312*, 71−74.
(36) Chen, Y. R., Sturgeon, B. E., Gunther, M. R., and Mason, R. P. (1999) Electron spin resonance investigation of the cyanyl and azidyl radical formation by cytochrome c oxidase. *J. Biol. Chem. 274*, 24611−24616.
(37) Musatov, A., Hebert, E., Carroll, C. A., Weintraub, S. T., and Robinson, N. C. (2004) Specific modification of two tryptophans within the nuclear-encoded subunits of bovine cytochrome c oxidase by hydrogen peroxide. *Biochemistry 43*, 1003−1009.
(38) Lemma-Gray, P., Weintraub, S. T., Carroll, C. A., Musatov, A., and Robinson, N. C. (2007) Tryptophan 334 oxidation in bovine cytochrome c oxidase subunit I involves free radical migration. *FEBS Lett. 581*, 437−442.
(39) Sedlak, E., Fabian, M., Robinson, N. C., and Musatov, A. (2010) Ferricytochrome c protects mitochondrial cytochrome c oxidase against hydrogen peroxide-induced oxidative damage. *Free Radical Biol. Med. 49*, 1574−1581.
(40) Musatov, A., and Robinson, N. C. (2012) Susceptibility of mitochondrial electron-transport complexes to oxidative damage. Focus on cytochrome c oxidase. *Free Radical Res. 46*, 1313−1326.
(41) Soulimane, T., and Buse, G. (1995) Integral cytochrome-c oxidase. Preparation and progress towards a three-dimensional crystallization. *Eur. J. Biochem. 227*, 588−595.
(42) Parul, D., Palmer, G., and Fabian, M. (2005) Proton interactions with hemes *a* and a_3 in bovine heart cytochrome c oxidase. *Biochemistry 44*, 4562−4571.
(43) Liao, G. L., and Palmer, G. (1996) The reduced minus oxidized difference spectra of cytochromes *a* and a_3. *Biochim. Biophys. Acta 1274*, 109−111.
(44) Buege, J. A., and Aust, S. D. (1978) Microsomal lipid peroxidation. *Methods Enzymol. 52*, 302−310.
(45) Bergmayer, H. U., Gawehn, K., and Grassl, M. (1970) H_2O_2. *Methoden Enzym. Anal. (3. Aufl.) 1*, 440.
(46) Andreae, W. A. (1955) A sensitive method for the estimation of hydrogen peroxide in biological materials. *Nature 175*, 859−860.
(47) Wikstrom, M., and Morgan, J. E. (1992) The dioxygen cycle. Spectral, kinetic, and thermodynamic characteristics of ferryl and peroxy intermediates observed by reversal of the cytochrome oxidase reaction. *J. Biol. Chem. 267*, 10266−10273.
(48) Bielski, B. H. J., Shiue, G. G., and Bajuk, S. (1980) Reduction of nitro blue tetrazolium by Co^{2-} and O^{2-} radicals. *J. Phys. Chem. 84*, 830−833.
(49) Altman, F. P., and Butcher, R. G. (1973) Studies on the reduction of tetrazolium salts. I. The isolation and characterisation of a half-formazan intermediate produced during the reduction of neotetrazolium chloride. *Histochemie 37*, 333−350.
(50) Kumar, C., Naqui, A., and Chance, B. (1984) Peroxide interaction with pulsed cytochrome oxidase. Optical and EPR studies. *J. Biol. Chem. 259*, 11668−11671.
(51) Pecoraro, C., Gennis, R. B., Vygodina, T. V., and Konstantinov, A. A. (2001) Role of the K-channel in the pH-dependence of the reaction of cytochrome c oxidase with hydrogen peroxide. *Biochemistry 40*, 9695−9708.
(52) Fabian, M., Skultety, L., Jancura, D., and Palmer, G. (2004) Implications of ligand binding studies for the catalytic mechanism of cytochrome c oxidase. *Biochim. Biophys. Acta 1655*, 298−305.
(53) Huang, C. (1969) Studies on phosphatidylcholine vesicles. Formation and physical characteristics. *Biochemistry 8*, 344−352.
(54) Lezerovich, A. (1986) Derivative UV spectra of lipid conjugated dienes. *J. Am. Oil Chem. Soc. 63*, 883−888.
(55) Igarashi, M., and Miyazawa, T. (2005) Preparation and fractionation of conjugated trienes from α-linolenic acid and their growth-inhibitory effects on human tumor cells and fibroblasts. *Lipids 40*, 109−113.
(56) Robinson, N. C., and Capaldi, R. A. (1977) Interaction of detergents with cytochrome c oxidase. *Biochemistry 16*, 375−381.
(57) Connor, H. D., Fischer, V., and Mason, R. P. (1986) A search for oxygen-centered free-radicals in the lipoxygenase linoleic-acid system. *Biochem. Biophys. Res. Commun. 141*, 614−621.

(58) Rosen, G. M., and Rauckman, E. J. (1981) Spin trapping of free radicals during hepatic microsomal lipid peroxidation. *Proc. Natl. Acad. Sci. U.S.A. 78*, 7346−7349.
(59) Oliveberg, M., Brzezinski, P., and Malmstrom, B. G. (1989) The effect of pH and temperature on the reaction of fully reduced and mixed-valence cytochrome c oxidase with dioxygen. *Biochim. Biophys. Acta 977*, 322−328.
(60) Oliveberg, M., and Malmstrom, B. G. (1992) Reaction of dioxygen with cytochrome c oxidase reduced to different degrees: Indications of a transient dioxygen complex with copper-B. *Biochemistry 31*, 3560−3563.
(61) Verkhovsky, M. I., Morgan, J. E., and Wikstrom, M. (1994) Oxygen binding and activation: Early steps in the reaction of oxygen with cytochrome c oxidase. *Biochemistry 33*, 3079−3086.
(62) Rigby, S. E., Junemann, S., Rich, P. R., and Heathcote, P. (2000) Reaction of bovine cytochrome c oxidase with hydrogen peroxide produces a tryptophan cation radical and a porphyrin cation radical. *Biochemistry 39*, 5921−5928.
(63) MacMillan, F., Kannt, A., Behr, J., Prisner, T., and Michel, H. (1999) Direct evidence for a tyrosine radical in the reaction of cytochrome c oxidase with hydrogen peroxide. *Biochemistry 38*, 9179−9184.
(64) Budiman, K., Kannt, A., Lyubenova, S., Richter, O. M., Ludwig, B., Michel, H., and MacMillan, F. (2004) Tyrosine 167: The origin of the radical species observed in the reaction of cytochrome c oxidase with hydrogen peroxide in *Paracoccus denitrificans*. *Biochemistry 43*, 11709−11716.
(65) MacMillan, F., Budiman, K., Angerer, H., and Michel, H. (2006) The role of tryptophan 272 in the *Paracoccus denitrificans* cytochrome c oxidase. *FEBS Lett. 580*, 1345−1349.
(66) Pinakoulaki, E., Pfitzner, U., Ludwig, B., and Varotsis, C. (2003) Direct detection of Fe(IV)═O intermediates in the cytochrome aa_3 oxidase from *Paracoccus denitrificans*/H_2O_2 reaction. *J. Biol. Chem. 278*, 18761−18766.
(67) Einarsdottir, O., Szundi, I., and Sucheta, A. (2002) P_M and P_R forms of cytochrome c oxidase have different spectral properties. *Biochemistry 91*, 87−93.
(68) Karpefors, M., Adelroth, P., Zhen, Y., Ferguson-Miller, S., and Brzezinski, P. (1998) Proton uptake controls electron transfer in cytochrome c oxidase. *Proc. Natl. Acad. Sci. U.S.A. 95*, 13606−13611.
(69) Faxen, K., Gilderson, G., Adelroth, P., and Brzezinski, P. (2005) A mechanistic principle for proton pumping by cytochrome c oxidase. *Nature 437*, 286−289.
(70) Smirnova, I. A., Zaslavsky, D., Fee, J. A., Gennis, R. B., and Brzezinski, P. (2008) Electron and proton transfer in the ba_3 oxidase from *Thermus thermophilus*. *J. Bioenerg. Biomembr. 40*, 281−287.
(71) Brzezinski, P., Ojemyr, L. N., and Adelroth, P. (2013) Intermediates generated during the reaction of reduced *Rhodobacter sphaeroides* cytochrome c oxidase with dioxygen. *Biochim. Biophys. Acta 1827*, 843−847.
(72) Chen, Y. R., Gunther, M. R., and Mason, R. P. (1999) An electron spin resonance spin-trapping investigation of the free radicals formed by the reaction of mitochondrial cytochrome c oxidase with H_2O_2. *J. Biol. Chem. 274*, 3308−3314.
(73) Vygodina, T. V., and Konstantinov, A. A. (2007) Peroxidase activity of mitochondrial cytochrome c oxidase. *Biochemistry (Moscow) 72*, 1056−64.
(74) Musatov, A. (2006) Contribution of peroxidized cardiolipin to inactivation of bovine heart cytochrome c oxidase. *Free Radical Biol. Med. 41*, 238−246.
(75) Musatov, A. (2013) Dual effect of heparin on Fe^{2+}-induced cardiolipin peroxidation: Implications for peroxidation of cytochrome c oxidase bound cardiolipin. *JBIC, J. Biol. Inorg. Chem. 18*, 729−737.
(76) Mitchell, R., and Rich, P. R. (1994) Proton uptake by cytochrome c oxidase on reduction and on ligand binding. *Biochim. Biophys. Acta 1186*, 19−26.
(77) Hosler, J. P., Shapleigh, J. P., Mitchell, D. M., Kim, Y., Pressler, M. A., Georgiou, C., Babcock, G. T., Alben, J. O., Ferguson-Miller, S., and Gennis, R. B. (1996) Polar residues in helix VIII of subunit I of cytochrome c oxidase influence the activity and the structure of the active site. *Biochemistry 35*, 10776−10783.
(78) Adelroth, P., Gennis, R. B., and Brzezinski, P. (1998) Role of the pathway through K(I-362) in proton transfer in cytochrome c oxidase from *R. sphaeroides*. *Biochemistry 37*, 2470−2476.
(79) Verkhovsky, M. I., Morgan, J. E., and Wikstrom, M. (1995) Control of electron delivery to the oxygen reduction site of cytochrome c oxidase: A role for protons. *Biochemistry 34*, 7483−7491.
(80) Ostermeier, C., Harrenga, A., Ermler, U., and Michel, H. (1997) Structure at 2.7 Å resolution of the *Paracoccus denitrificans* two-subunit cytochrome c oxidase complexed with an antibody FV fragment. *Proc. Natl. Acad. Sci. U.S.A. 94*, 10547−10553.
(81) Svensson-Ek, M., Abramson, J., Larsson, G., Tornroth, S., Brzezinski, P., and Iwata, S. (2002) The X-ray crystal structures of wild-type and EQ(I-286) mutant cytochrome c oxidases from *Rhodobacter sphaeroides*. *J. Mol. Biol. 321*, 329−339.
(82) Yoshikawa, S., Shinzawa-Itoh, K., Nakashima, R., Yaono, R., Yamashita, E., Inoue, N., Yao, M., Fei, M. J., Libeu, C. P., Mizushima, T., Yamaguchi, H., Tomizaki, T., and Tsukihara, T. (1998) Redox-coupled crystal structural changes in bovine heart cytochrome c oxidase. *Science 280*, 1723−1729.
(83) Adelroth, P., Ek, M. S., Mitchell, D. M., Gennis, R. B., and Brzezinski, P. (1997) Glutamate 286 in cytochrome aa_3 from *Rhodobacter sphaeroides* is involved in proton uptake during the reaction of the fully-reduced enzyme with dioxygen. *Biochemistry 36*, 13824−13829.
(84) Konstantinov, A. A., Siletsky, S., Mitchell, D., Kaulen, A., and Gennis, R. B. (1997) The roles of the two proton input channels in cytochrome c oxidase from *Rhodobacter sphaeroides* probed by the effects of site-directed mutations on time-resolved electrogenic intraprotein proton transfer. *Proc. Natl. Acad. Sci. U.S.A. 94*, 9085−9090.